# A Dual-Band Self-Oscillating Mixer for $C$-Band and $X$-Band Applications

Brad R. Jackson, *Student Member, IEEE*, and Carlos E. Saavedra, *Senior Member, IEEE*

***Abstract*—A self-oscillating mixer that employs both the fundamental and harmonic signals generated by the oscillator subcircuit in the mixing process is experimentally demonstrated. The resulting circuit is a dual-band down-converting mixer that can operate in $C$-band from 5.0 to 6.0 GHz, or in $X$-band from 9.8 to 11.8 GHz. The oscillator uses active superharmonic coupling to enforce the quadrature relationship of the fundamental outputs. Either the fundamental outputs of the oscillator or the second harmonic oscillator output signals that exists at the common-mode nodes are connected to the mixer via a set of complementary switches. The mixer achieves a conversion gain between 5–12 dB in both frequency bands. The output 1-dB compression points for both modes of the mixer are approximately −5 dBm and the output third-order intercept point for $C$-band and $X$-band operation are 12 and 13 dBm, respectively. The integrated circuit was fabricated in 0.13-$\mu$m CMOS technology and measures 0.525 mm$^2$ including bonding pads.**

***Index Terms*—Dual-band mixer, harmonic self-oscillating mixer (SOM), quadrature oscillator, subharmonic mixer.**

## I. Introduction

THE DESIRE to realize multifunction wireless communications devices has led to an interest in designing circuits that operate in multiple bands in an attempt to avoid requiring a duplication of the RF circuitry. Often in multiband wireless communications systems, there is a separate RF front-end for each frequency band of operation, consisting of multiple low-noise amplifiers, mixers, and oscillators. Clearly there is significant potential to reduce power consumption and chip area required if some of the RF front-end circuits can be used for more than one frequency band.

There have been several demonstrations of dual-band mixer circuits. For example, in [1], a switched inductor matching network was used to match the input impedance in the two bands of interest. Similarly, in [2], an *L–C* network was used to achieve input and output matching simultaneously in the two desired bands. In [3], a dual-band front-end was demonstrated, but used redundant circuitry as opposed to realizing a dual-band mixer with a single mixer core. A dual-band upconverter was discussed in [4], but also used two mixer cores. In each of these previous designs, multiple local oscillators (LOs) were used or an external LO signal was used as the input to the mixer.

Manuscript received February 04, 2009; revised August 19, 2009. First published January 19, 2010; current version published February 12, 2010. This work was supported in part by the Ontario Centres of Excellence (OCE) and by the Natural Sciences and Engineering Research Council of Canada (NSERC).

B. R. Jackson is with the Department of Electrical and Computer Engineering, Royal Military College of Canada, Kingston, ON, Canada K7K 7B4 (e-mail: Brad.Jackson@rmc.ca).

C. E. Saavedra is with the Department of Electrical and Computer Engineering, Queen's University, Kingston, ON, Canada K7L 3N6 (e-mail: Carlos.Saavedra@queensu.ca).

Digital Object Identifier 10.1109/TMTT.2009.2037865

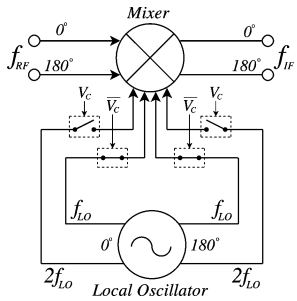


Fig. 1. Block diagram of the proposed dual-band SOM.

In this paper, a fully integrated dual-band self-oscillating mixer (SOM) circuit is demonstrated that uses a single oscillator and a single mixer core. The dual-band performance is achieved by usefully exploiting the fundamental *and* harmonic signals that are generated by the oscillator subcircuit. In other words, this circuit can function either as a fundamental-mode SOM or as a subharmonic SOM. While there have been previous studies on subharmonic SOMs [5]–[7] and many more on fundamental-mode SOMs, to the best of our knowledge, this study describes the first chip that incorporates both types of SOMs in a single design. As a demonstration of this technique, a chip was fabricated using CMOS 0.13 $\mu$m technology with dual-band operation in $C$-band and $X$-band. Measurement results are shown that characterize the gain and linearity of the circuit in both states of operation.

## II. Circuit Description

A block diagram of the proposed dual-band SOM is shown in Fig. 1. This figure shows a downconverting mixer with differential RF input and IF output, as well as a reconfigurable LO input. If an LO is available that has a differential output at both $f_{\rm LO}$ and $2f_{\rm LO}$, two pairs of complementary switches can be used to connect the desired LO signal to the mixer. Depending on the state of the switches, the mixer can have an LO input in two different frequency bands, thus permitting two different RF frequency bands at the mixer input while maintaining a constant IF output. The result is a dual-band SOM using a single on-chip quadrature voltage-controlled oscillator (VCO) along with a single mixer circuit. To distinguish between the two states of the dual-band SOM, the term "fundamental mode" will be used to describe the circuit state where the fundamental oscillator output at $f_{\rm LO}$ is connected to the mixer, and the term "subharmonic mode" will be used to describe the state where the $2f_{\rm LO}$ signal is connected to the mixer.

There are many types of mixers that have a broadband frequency response. That frequency response, however, is narrowed by the baluns and impedance-matching circuitry that are used to interface with the mixer. In the case of SOMs, the intrinsic broadband response of the mixer is restricted not only by the interface circuitry, but more importantly by the tuning range of the oscillator subcircuit. The design approach used in this paper noticeably extends the useful bandwidth of the SOM because feeding the mixer stage with the second harmonic of the VCO in addition to the fundamental tone expands the operating frequency band of the SOM by a factor of 3. To see how this occurs, note that, in the fundamental mode, the VCO has a tuning range of $\Delta\omega$, but at the second harmonic, the frequency swing is doubled to $2\Delta\omega$. Since the tuning range of the oscillator is the determining factor in the frequency response of the chip, the *aggregate* bandwidth of this SOM is now $\Delta\omega + 2\Delta\omega = 3\Delta\omega$.

### A. Voltage-Controlled Quadrature Oscillator

The general topology chosen for the oscillator in this study is the well-known cross-coupled pair oscillator. This basic oscillator circuit uses two cross-coupled transistors to generate a negative resistance equal to $-2/g_m$ that is used to counteract the losses in the *L–C* tank. The output of this oscillator is differential at the drains of the two cross-coupled field-effect transistors (FETs). In order to use this technique to realize a quadrature oscillator, two identical cross-coupled oscillator circuits can be used along with a connecting circuit that enforces a quadrature relationship between the fundamental outputs. There have been several techniques proposed to enforce quadrature outputs including fundamental coupling circuits [8] and superharmonic coupling circuits [9]–[13]. Superharmonic coupling exploits the existence of even-ordered harmonic signals at the common-mode nodes of an oscillator, the strongest of which is at twice the fundamental frequency. By enforcing a 180° relationship between the second harmonic signals in the two otherwise separate oscillator circuits, a quadrature relationship between the fundamental outputs is obtained. Superharmonic coupling was the natural choice for this work since the second-harmonic signal will also be used for the mixer while in the subharmonic mode. Superharmonic coupling can be achieved using both passive [9]–[11] and active [12], [13] techniques. Active superharmonic coupling was used for the quadrature oscillator in this study because of its significant advantage of requiring much less space on-chip by replacing the transformer with a cross-coupled pair of FETs.

The voltage-controlled quadrature oscillator circuit is shown in Fig. 2. Each of the two cross-coupled oscillators will oscillate at the same frequency $f_{\rm LO} = 1/(2\pi\sqrt{2LC_{\rm tot}})$, where $L$ is the inductance shown in Fig. 2, and $C_{\rm tot}$ is the total capacitance including the varactor capacitance $C$, as well as any parasitic capacitance at the output nodes. The nodes labelled *CM1* and *CM2* in Fig. 2 are examples of common-mode nodes where only the even-order harmonics of the fundamental outputs exist, the most dominant of which is the second harmonic at $2f_{\rm LO}$. An additional cross-coupled pair is used to connect the two oscillators and generate a 180° relationship between the second-order harmonic signals at *CM1* and *CM2*, which enforces a quadrature

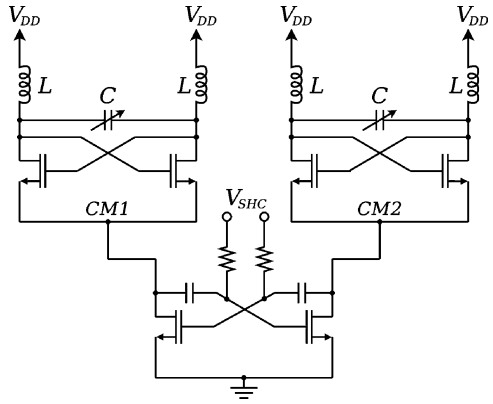


Fig. 2. Quadrature VCO using superharmonic coupling.

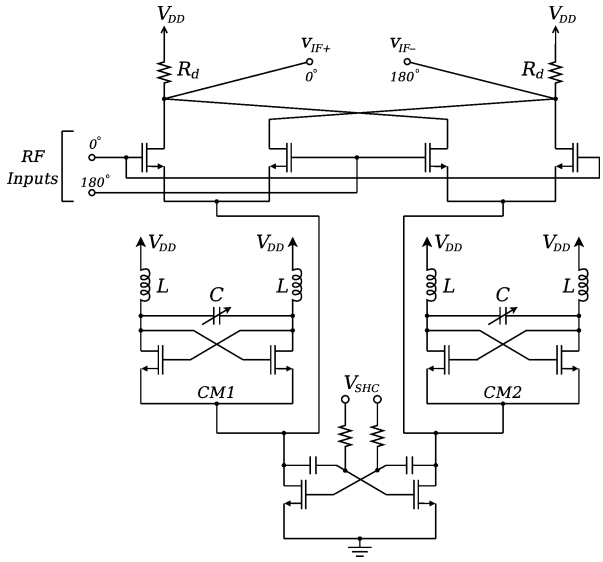


Fig. 3. Simplified circuit schematic of the proposed dual-band SOM in subharmonic mode.

relationship between the fundamental outputs. The frequency of the oscillator is tuned via a control voltage on the varactor shown in Fig. 2. An advantage of using the second-harmonic signal for the mixer while in the subharmonic mode is the doubling of the tuning range of the oscillator compared to the fundamental tuning range. Compared to the quadrature oscillator in [13], this oscillator does not use cross-coupled PMOS transistors above the cross-coupled NMOS transistors in order to maximize the $2f_{\rm LO}$ signal at the common-mode nodes *CM1* and *CM2*.

The bias voltage on the gates of the coupling circuit $V_{SHC}$ is set to strongly couple the $2f_{\rm LO}$ signal to ensure a differential relationship is established at *CM1* and *CM2* when the oscillator reaches a steady-state, thus resulting in quadrature fundamental outputs. Source–follower buffers were connected to the four fundamental outputs of the quadrature oscillator (not shown in Fig. 2) so that the effect of connecting the oscillator output to other circuits will be minimal. To reduce the overall power consumption of the proposed dual-band SOM, any low-power buffer circuit architecture could be used to connect the output of the oscillator to the mixer or even straightforward differential pairs. Furthermore, the buffer circuits could be shut off while

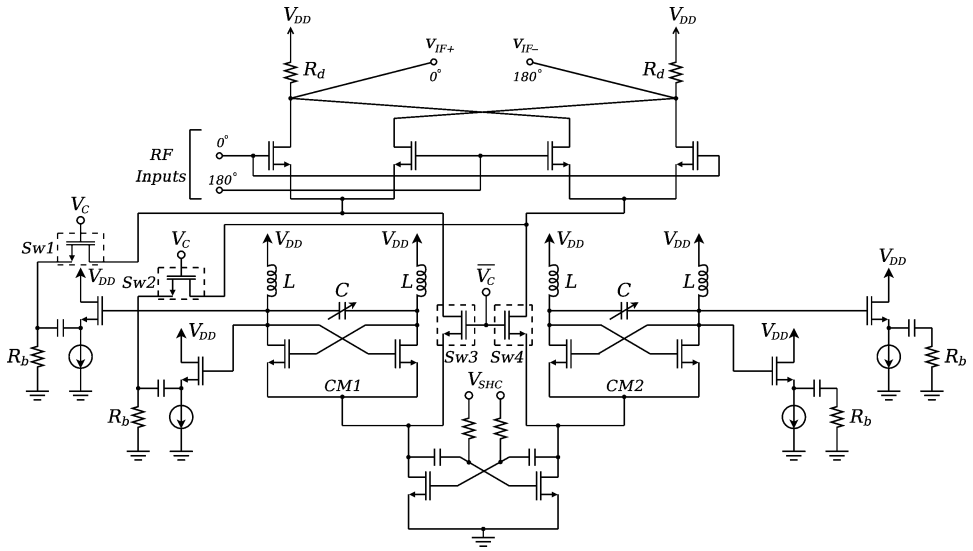


Fig. 4. Circuit schematic of the proposed dual-band SOM.

the circuit is in the subharmonic mode by simply controlling the gate–voltage on the buffer transistors, which could result in a significant power savings.

### B. Mixer

The mixer circuit uses the top half of the traditional Gilbert-cell topology. Fig. 3 shows a simplified circuit schematic of the mixer in the subharmonic mode. The common-mode nodes where the second harmonic signal is dominant is connected to the sources of the RF transistors.

These $2f_{\rm LO}$ signals at *CM1* and *CM2* are 180° out of phase with each other, which maintains the double-balanced characteristic of the Gilbert cell. The circuit could be implemented as shown in Fig. 3 as a single-band mixer with the doubled LO frequency output. If implemented in this way, the use of an additional frequency doubler circuit connected to the fundamental output could be avoided, thus saving chip space and reducing power consumption.

A simplified circuit diagram of the dual-band SOM is shown in Fig. 4. Included in this figure are the four source–follower buffers that are connected to the fundamental quadrature oscillator output. The value of $R_b$ was selected to equalize the fundamental signal amplitude with the $2f_{\rm LO}$ signal amplitude at *CM1* and *CM2*. To select the fundamental mode for the mixer, the control voltage $V_C$ is set to $V_{DD}$, turning on switches $Sw1$ and $Sw2$ and turning off switches $Sw3$ and $Sw4$. This connects the 0° and 180° fundamental outputs at $f_{\rm LO}$ to the sources of the RF transistors. The 90° and 270° fundamental outputs are connected to identical source–follower buffers as the 0° and 180° outputs to maintain equal loads to the oscillator tank. Note that the 90° and 270° fundamental outputs of the oscillator are not used in the fundamental mode of operation; however, they are required to generate the $2f_{\rm LO}$ signal at *CM2* for the subharmonic mode, and they could be used elsewhere in the system if needed. For the subharmonic mode, the control voltage $V_C = 0$ V, turning off switches $Sw1$ and $Sw2$, and turning on switches $Sw3$ and $Sw4$. This connects the 0° and 180° $2f_{\rm LO}$ signals to the sources of the RF transistors.

Each of the two outputs of the mixer at $V_{\rm IF+}$ and $V_{\rm IF-}$ are connected to source–follower buffers and connected to bonding pads. These two signals are combined off-chip and connected to the 50-Ω measurement equipment. The source–follower buffers and combiner were designed such that the output voltage amplitude across the $50-\Omega$ load of the measurement equipment is equal to $(V_{\rm IF+} - V_{\rm IF-})$.

Alternative circuit configurations are possible to achieve a similar behavior to that presented in this study. For example, an oscillator whose fundamental frequency is $2f_{\rm lo}$ followed by a frequency divider to generate the $f_{\rm lo}$ signal could be used. While the quadrature oscillator approach employed here does lead to a certain overhead in dc power dissipation due to the need for two oscillators, using the frequency-divider method would not necessarily bring significant savings in dc power since frequency dividers can easily consume as much power as a single oscillator.

Another possible configuration is to only use the fundamental outputs of the quadrature oscillator along with the subharmonic mixer described in [14] and [15]. In that type of subharmonic mixer, the four transistors in the LO path require quadrature inputs at 0°, 90°, 180°, and 270°, which is precisely what the quadrature oscillator provides. In order to achieve dual-band operation, a series of switches are needed to connect the 0°, 90°, 180°, and 270° signals to the appropriate LO transistors for the subharmonic mode, and only connect the 0° and 180° to the appropriate LO transistors for the fundamental mode. It was found through simulation that greater conversion gain could be achieved by directly using the doubled frequency component already present at the common mode as opposed to using the quadrature fundamental outputs with an LO doubling pair. Furthermore, a lower noise figure was obtained by using the $2f_{\rm LO}$ signal directly from the oscillator due to the elimination of the switching noise that accompanies the LO doubling pairs in the subharmonic mixer topology of [14] and [15].

## III. Measurement Results

The dual-band SOM was characterized using coplanar-waveguide probes, signal sources, and a spectrum analyzer. The

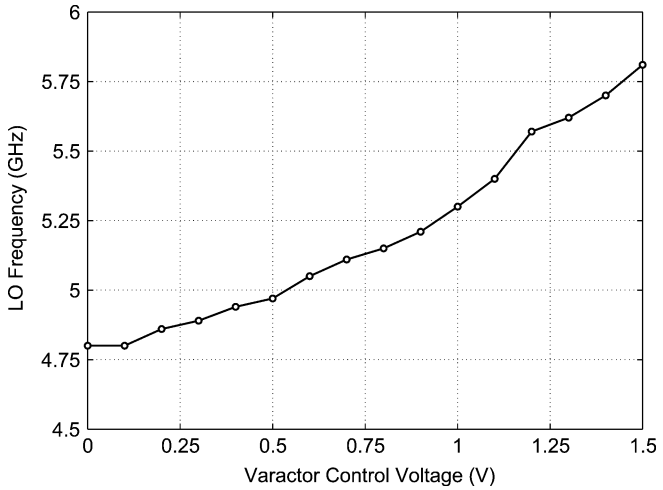


Fig. 5. Measured fundamental LO frequency tuning for $V_{\rm cap} = 0 - 2.4$ V.

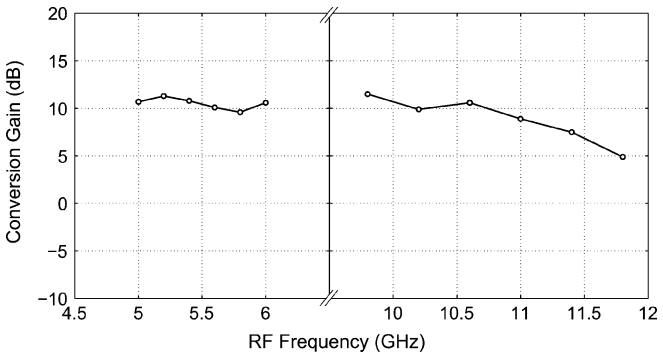


Fig. 6. Conversion gain at various RF input frequencies for a fixed IF frequency of 200 MHz.

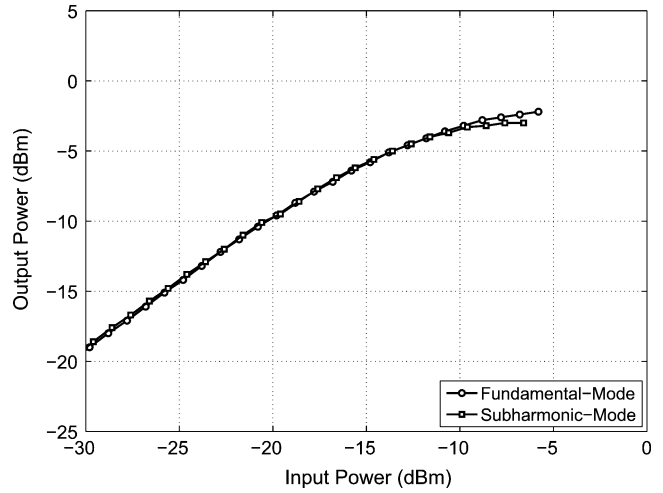


Fig. 7. Measured IF output power at 200 MHz for various RF input power levels for both fundamental mode ($\rm RF = 5.0$ GHz) and subharmonic mode ($\rm RF = 9.8$ GHz).

supply voltage $V_{DD}$ was set to 1.5 V. The fundamental oscillation frequency was measured at various varactor control voltages $V_{\rm cap}$, and the results are shown in Fig. 5. As shown in this figure, the oscillation frequency can be tuned from 4.8 to 5.8 GHz as $V_{\rm cap}$ is varied from 0 to 1.5 V. When the circuit

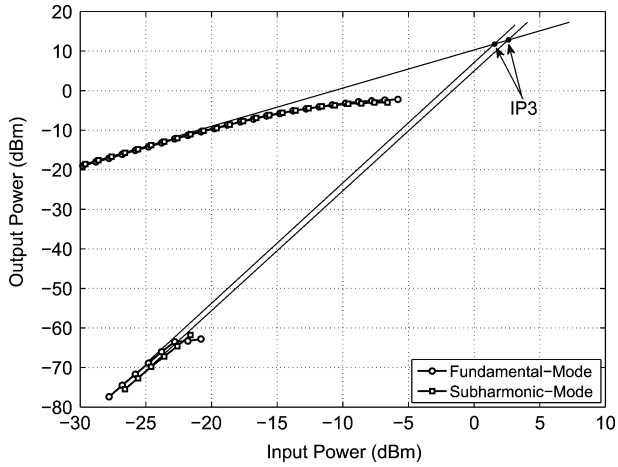


Fig. 8. IM3 measurement for both fundamental and subharmonic mixer modes.

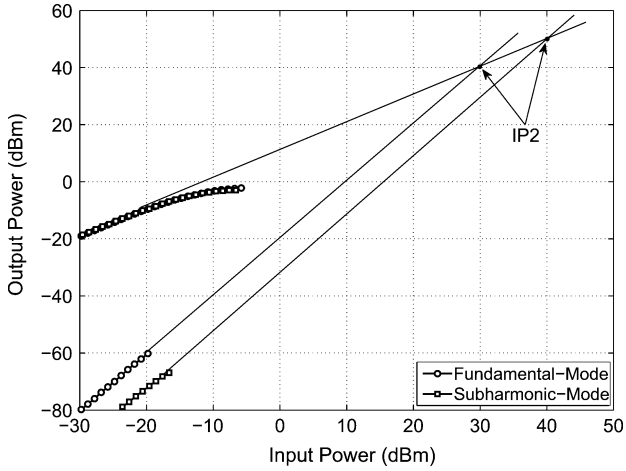


Fig. 9. IM2 measurement for both fundamental and subharmonic mixer modes.

TABLE I
FUNDAMENTAL-MODE AND SUBHARMONIC-MODE LO FEEDTHROUGH MEASUREMENTS

| | Fundamental-Mode (dBm) | Subharmonic-Mode (dBm) |
|---|---|---|
| $f_{LO}$ @ RF | -40.3 | -36.7 |
| $2f_{LO}$ @ RF | -25.1 | -35.6 |
| $f_{LO}$ @ IF | -47.5 | -48.4 |
| $2f_{LO}$ @ IF | -58.9 | -46.1 |

is in the subharmonic mode, this output frequency is doubled, thus giving an LO frequency range from 9.6 to 11.6 GHz.

The conversion gain of the mixer was measured in both states at various LO frequencies and the results are shown in Fig. 6. An IF frequency of 200 MHz was used, giving an RF input frequency range from 5.0 to 6.0 GHz and 9.8 to 11.8 GHz for the fundamental and subharmonic modes, respectively. Fig. 6 shows a power conversion gain of between approximately 10 and 12 dB for the fundamental mode of the mixer, and a range from 5 to 12 dB for the subharmonic mode. The decrease in conversion gain at higher RF frequencies for the subharmonic mode is due

TABLE II
COMPARISON OF HARMONIC SOMs

| Reference | Frequency (GHz) | Bandwidth (GHz) | Harmonic Number | Conversion Gain (dB) | Power Consumption (mW) | Noise Figure (dB) | Dual-Band? |
|---|---|---|---|---|---|---|---|
| [5] | 10.6 – 11.8 | 1.2 | 3 | 2.5 | 43 | – | No |
| [6] | 5.8 | – | 3 | 11.1 | 32 | 6.9 | No |
| [7] | 70 – 85 | 15 | 2 | –15 | – | – | No |
| **This Work** | **5 – 6 9.8 – 11.8** | **3.0** | **1 and 2** | **5 – 12** | **68** | **8.7 – 10.9** | **Yes** |

to parasitic capacitances reducing the $2f_{\mathrm{LO}}$ signal amplitude as the frequency is increased. Since the input RF signal to the circuit is applied directly to the gates of MOSFETs, as shown in Fig. 4, the input is not matched to a 50-$\Omega$ system. This situation would likely be the case when the mixer is a subcircuit of a larger RF integrated circuit (RFIC). The *voltage* conversion gain of the mixer is approximately 6 dB lower than shown in Fig. 6.

The RF power performance of the circuit was measured using a fixed LO fundamental frequency of 4.8 GHz ($2f_{\mathrm{LO}} = 9.6$ GHz), the input RF power was varied, and the output power of the IF signal was measured. The results of the fundamental-mode measurement with an RF frequency of 5.0 GHz and the subharmonic-mode measurements with an RF frequency of 9.8 GHz are shown in Fig. 7. The two curves are very similar, and the output 1-dB compression points both occur at $-5$ dBm.

The third-order intermodulation (IM3) products were also measured using two-tone RF inputs of 5.00 and 5.02 GHz for the fundamental mode, and 9.80 and 9.82 GHz for the subharmonic mode (IM3 signals at 180 and 240 MHz). The results, shown in Fig. 8, display an output third-order intercept point (OIP3) of 12 dBm for the fundamental mode and 13 dBm for the subharmonic mode. The second-order intermodulation (IM2) products were also measured at an IM2 signal frequency of 20 MHz, and the results are shown in Fig. 9. The mixer demonstrates strong linearity with an output second-order intercept point (OIP2) of 40 dBm in fundamental mode and an OIP2 of 50 dBm for the subharmonic mode.

The LO feedthrough was measured at the RF and IF ports and the results are shown in Table I. This table shows the output power levels of the $f_{\mathrm{LO}}$ and $2f_{\mathrm{LO}}$ signals at the RF and IF ports for an LO fundamental frequency of 4.8 GHz. In fundamental mode, the LO signal at the RF port is $-40.3$ dBm, which is an isolation of approximately 40 dB since the oscillator output signal has a power of approximately 0 dBm from simulations. Similarly, the $2f_{\mathrm{LO}}$ signal at the RF port for subharmonic mode shows about 36 dB of isolation.

The RF to IF isolation was measured to be 35 dB for both mixer states.

Since the switches are not ideal, some of the $2f_{\mathrm{LO}}$ signal will leak into the mixer while it is in the fundamental state and some of the $f_{\mathrm{LO}}$ signal will leak to the mixer in the subharmonic state. The conversion gain from the undesired LO signal was measured to evaluate the mixer performance in this regard. With the mixer in the fundamental mode ($f_{\mathrm{LO}} = 4.8$ GHz), an RF signal input of $-25$ dBm at 9.8 GHz was used and the power of the output signal at 200 MHz was measured. Ideally, there should be no power at this frequency, but since some of the $2f_{\mathrm{LO}}$ signal at 9.6 GHz leaks to the mixer, it will produce a 200-MHz IF output from the 9.8-GHz RF signal. The conversion gain for this case was $-15.2$ dB. Similarly, with the mixer in the subharmonic mode, an RF input of $-25$ dBm at 5.0 GHz was used to measure the conversion gain due to the leakage of the fundamental LO signal at 4.8 GHz. The conversion gain for this case was $-19.7$ dB. In both cases, the conversion gain is more than 20 dB below the conversion gain from the desired LO signal. The leakage can be made smaller by using a switch with higher isolation. An example of such a switch is a three-transistor network arranged in a $\pi$ configuration.

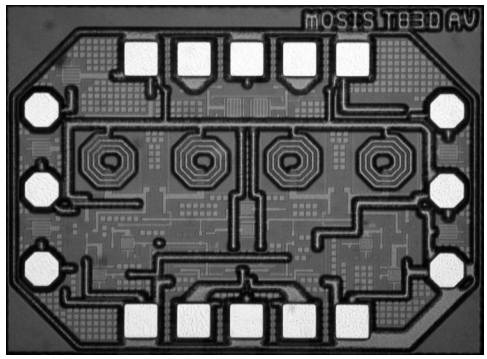


Fig. 10. Microphotograph of the dual-band SOM chip.

The phase noise of the VCO could not be measured because there were no pads connected to the oscillator output. However, the DSB noise figure was measured for the mixer in both states and was found to be 8.7 dB for fundamental mode and 10.9 dB for subharmonic mode. The dc power consumption of the quadrature oscillator alone was measured to be 68 mW including the four buffers. The buffers that are connected to the fundamental outputs of the oscillator consume a total of approximately 48 mW (12 mW each). The mixer circuit adds an additional 2 mW approximately in both the fundamental and subharmonic states. A comparison is shown in Table II, which shows the performance of this work along with several harmonic SOMs. The proposed architecture has the largest bandwidth while also achieving conversion gain. A microphotograph of the fabricated chip is shown in Fig. 10. The dimensions of the chip were 875 $\mu$m $\times$ 600 $\mu$m (0.525 mm$^2$) including bonding pads.

## IV. Conclusion

A new topology for a dual-band SOM has been demonstrated using CMOS 0.13-$\mu$m technology. This technique uses both the fundamental and second harmonic outputs of a single on-chip quadrature VCO connected to a mixer through complementary switches. For $C$-band operation, switches connect the fundamental oscillator output to the mixer, and for $X$-band operation, switches connect the second harmonic of the oscillator to the mixer. The mixer achieves a conversion gain of at least 5 dB over RF frequencies of 5.0 to 6.0 GHz and from 9.8 to 11.8 GHz while maintaining a constant IF output. This circuit could be used as part of a multistandard system on a chip to reduce the number of circuit elements required, potentially resulting in lower power consumption and reduced costs. This technique could also be very attractive at millimeter-wave frequencies where the use of a frequency-doubler circuit connected to the output of an LO could be avoided and in cases where the use of a broadband mixer circuit is not possible.

## References


[1] Y.-S. Hwang *et al.*, "A 2 GHz and 5 GHz dual-band direct conversion RF frontend for multi-standard applications," in *Proc. IEEE Int. SOC Conf.*, Sep. 2005, pp. 189–192.

[2] T. Abdelrheem, H. Elhak, and K. Sharaf, "A concurrent dual-band mixer for 900 MHz/1.8 GHz RF front-ends," in *Proc. 46th IEEE Int. Midwest Circuits Syst. Symp.*, Dec. 2003, vol. 3, pp. 1291–1294.

[3] W. Kim *et al.*, "A dual-band RF front-end of direct conversion receiver for wireless CDMA cellular phones with GPS capability," *IEEE Trans. Microw. Theory Tech.*, vol. 54, no. 5, pp. 2098–2105, May 2006.

[4] M. Arasu *et al.*, "A 3 to 9-GHz dual-band up-converter for a DS-UWB transmitter in 0.18-$\mu$m CMOS," in *IEEE Radio Freq. Integr. Circuits Symp.*, Jun. 2007, pp. 497–500.

[5] M. Fernandez *et al.*, "Nonlinear optimization of wide-band harmonic self-oscillating mixers," *IEEE Microw. Wireless Compon. Lett.*, vol. 18, no. 5, pp. 347–349, May 2008.

[6] S. W. Winkler *et al.*, "Integrated receiver based on a high-order subharmonic self-oscillating mixer," *IEEE Trans. Microw. Theory Tech.*, vol. 55, no. 6, pp. 1398–1404, Jun. 2007.

[7] M. Roberts, S. Iezekiel, and C. Snowden, "A $W$-band self-oscillating subharmonic MMIC mixer," *IEEE Trans. Microw. Theory Tech.*, vol. 46, no. 12, pp. 2104–2108, Dec. 1998.

[8] A. Rofougaran *et al.*, "A single-chip 900-MHz spread-spectrum wireless transceiver in 1-$\mu$m CMOS. I. Architecture and transmitter design," *IEEE J. Solid-State Circuits*, vol. 33, no. 4, pp. 515–534, Apr. 1998.

[9] J. Cabanillas, L. Dussopt, J. Lopez-Villegas, and G. Rebeiz, "A 900 MHz low phase noise CMOS quadrature oscillator," in *IEEE Radio Freq. Integr. Circuits Symp.*, 2002, pp. 63–66.

[10] C. Meng, Y. Chang, and S. Tseng, "4.9-GHz low-phase-noise transformer-based superharmonic-coupled GaInP/GaAs HBT QVCO," *IEEE Microw. Wireless Compon. Lett.*, vol. 16, no. 6, pp. 339–341, Jun. 2006.

[11] S. Gierkink *et al.*, "A low-phase-noise 5-GHz CMOS quadrature VCO using superharmonic coupling," *IEEE J. Solid-State Circuits*, vol. 38, no. 7, pp. 1148–1154, Jul. 2003.

[12] T. Hancock and G. Rebeiz, "A novel superharmonic coupling topology for quadrature oscillator design at 6 GHz," in *IEEE Radio Freq. Integr. Circuits Symp. Dig.*, Jun. 2004, pp. 285–288.

[13] B. R. Jackson and C. E. Saavedra, "A 3 GHz CMOS quadrature oscillator using active superharmonic coupling," in *Eur. Microw. Conf.*, Oct. 2007, pp. 1109–1112.

[14] K. Nimmagadda and G. Rebeiz, "A 1.9 GHz double-balanced subharmonic mixer for direct conversion receivers," in *IEEE Radio Freq. Integr. Circuits Symp., Dig.*, 2001, pp. 253–256.

[15] B. R. Jackson and C. E. Saavedra, "A CMOS subharmonic mixer with input and output active baluns," *Microw. Opt. Technol. Lett.*, vol. 48, pp. 2472–2478, Dec. 2006.


**Brad R. Jackson** (S'05) received the B.Sc. (Eng.) degree in electrical engineering, M.Sc. (Eng.) degree, and Ph.D. degree in electrical engineering from Queen's University, Kingston, ON, Canada, in 2002, 2005, and 2009, respectively.

He is currently a Postdoctoral Fellow with the Royal Military College of Canada, Kingston, ON, Canada. His research interests are in the field of RF CMOS and RF microelectromechanical systems (MEMS) integrated circuits such as mixers, filters, low-noise amplifiers (LNAs), frequency dividers, and frequency multipliers, as well as antennas and radar systems.

Dr. Jackson is a member of the IEEE Microwave Theory and Techniques Society (IEEE MTT-S).

**Carlos E. Saavedra** (S'92–M'98–SM'05) received the Ph.D. degree in electrical engineering from Cornell University, Ithaca, NY, in 1998.

From 1998 to 2000, he was with the Millitech Corporation, South Deerfield, MA. Since August 2000, he has been with the Department of Electrical and Computer Engineering, Queen's University, Kingston, ON, Canada, where he is currently an Associate Professor and the Coordinator of Graduate Studies. His research interests are in the field of microwave integrated circuits and systems for communications, automotive, and biological applications.

Dr. Saavedra is a Registered Professional Engineer (P. Eng.) in the Province of Ontario. He is the vice-chair of the MTT TCC-22 and is a member of the Technical Program Committee of the IEEE RFIC Symposium.